On the Extensional Rheology of Polymer Melts and Concentrated Solutions

ARTICLE *in* MACROMOLECULES · DECEMBER 2013

Impact Factor: 5.8 · DOI: 10.1021/ma401213r

4 AUTHORS, INCLUDING:

Tam Sridhar
Monash University (Australia)
104 PUBLICATIONS **2,517** CITATIONS
SEE PROFILE

Daniel Nguyen
GTI NetCorp
411 PUBLICATIONS **10,558** CITATIONS
SEE PROFILE

Pradipto Bhattacharjee
Monash University (Australia)
26 PUBLICATIONS **178** CITATIONS
SEE PROFILE

Macromolecules

Article

pubs.acs.org/Macromolecules

On the Extensional Rheology of Polymer Melts and Concentrated Solutions

T. Sridhar,* Mohini Acharya, D. A. Nguyen, and P. K. Bhattacharjee

Department of Chemical Engineering, Monash University, Clayton, Victoria 3800, Australia

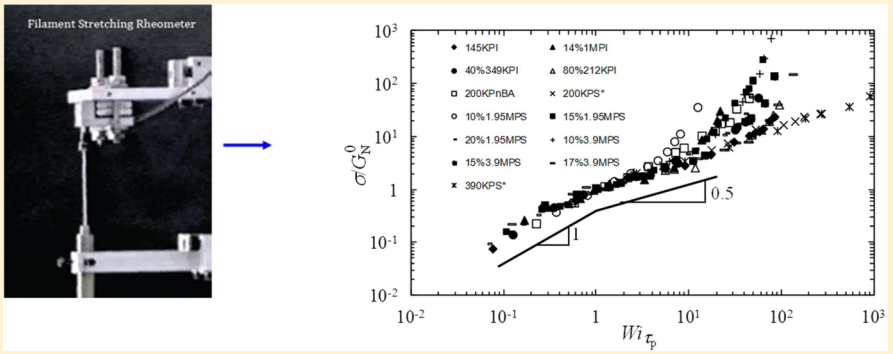

ABSTRACT: We examine the influence of the number of entanglements per chain (Z) on the uniaxial extensional rheology of polymer melts and concentrated solutions. We subject fluids with wide range of Z (13−51) to uniaxial extensional flow at strain rates that also spans a wide range: starting at strain rates that much less than the inverse of the longest measurable relaxation time of the chains to strain rates that are in excess of the order of the inverse of the Rouse time of the chain. The results show that the value of Z critically influences extensional flow at all strain rates examined. The combination of results presented here and those from recent literature clearly establish areas where the agreement between tube theory and experiments is less than satisfactory. These differences are particularly evident at strain rates wherein chain stretching is expected to play a role. There are also differences in the behavior of polystyrene melts and other systems investigated. Taking together exiting data indicate that the universality of the tube model may break down at large strain rates. It is possible that the monomeric friction coefficient depends sensitively on molecular architecture and the surrounding environment. The presence of pendant groups on the monomer background may influence the friction coefficient. Predicting this *apriori* remains a challenge. Additionally we show that the parameter λ_{max}/Z, where λ_{max} is the ratio of the maximum length of a polymer chain to its equilibrium length, influences the flow behavior to the extent that fluids having equal values of λ_{max}/Z demonstrate similar rheological behavior at all deformation rates when the extensional flow response is suitably scaled. We also compare our results with those obtained on other polymer melts in uniaxial extensional flow reported previously in literature.

I. INTRODUCTION

The flow properties of entangled polymer melts and concentrated solutions have in recent years been mostly considered using the framework of the Doi−Edwards model.[1] Several modifications of the original model have been made to improve the predictions of the model, and a large number of mechanisms what the original model did not possess have now been included in the framework. Current models dealing with the dynamics of this class of fluids predict an extensional rheological response that consist of four regimes depending on how the imposed extension rate compares with the longest measurable relaxation time (τ_d^f) and the Rouse time (τ_R) of the chains. The most recent versions of the model suggest that in Regime 1, where the extensional strain-rate ($\dot{\varepsilon}$) is less than the inverse of τ_d^f the extensional viscosity assumes a value of $3\eta_0$ where η_0 is the zero shear rate viscosity. In this range the stress (σ) scales linearly with the strain-rate. In Regime 2, where $1/\tau_d^f \leq \dot{\varepsilon} < 1/\tau_R$, the extensional viscosity (η_E) decreases as $\dot{\varepsilon}^{-1}$. In regime 3, where $\dot{\varepsilon} > 1/\tau_R$, η_E and σ rapidly increase above the limiting value of $3\eta_0$ and 3 G_N^0 respectively, where G_N^0 is the plateau modulus. Finally, in Regime 4, η_E saturates at a constant value which is predicted by a recent model to be of magnitude $6\eta_0\lambda_{max}^2/(1 + 1.5Z)$ as $\dot{\varepsilon} \to \infty$,[2] where λ_{max} is the ratio of the maximum length of a polymer chain to its equilibrium length. While it is clear that the functional relationship between η_E and σ on strain-rate ($\dot{\varepsilon}$) is governed by Z, η_0 and λ_{max} the form of these relationships change with different models especially in regime 2 and regime 3. In particular, in regime 3, a rapid increase in the extensional viscosity has been observed in majority of experiments involving entangled solutions of polystyrene.[3] However in identical experiments[4] conducted on entangled melts of polystyrene of two different molecular weights, the extensional viscosity in regime 3 has been observed to continue to decrease with increasing strain-rate. The

Received: June 20, 2013
Revised: December 15, 2013
Published: December 30, 2013

   dx.doi.org/10.1021/ma401213r | *Macromolecules* 2014, 47, 379−386

Table 1. Material Parameters and Properties of Fluids at 21.5 °C

name	polymer	M_w [g/mol]	c [wt %]	Z	η_0 [Pa·s]	G_N^0 [Pa]	λ_{max}	τ_d^f [s]	τ_R [s]	τ_p [s]	τ_d^f/τ_R	λ_{max}/Z
200 KPnBA	poly(*n*-butyl acrylate)	209 600	100	13.1	32 800	131 060	4.1	0.79	0.069	0.8	11.4	0.31
10%1.95MPS	polystyrene	1 950 000	10	15	368	1706	13.1	0.64	0.047	0.78	13.6	0.87
200 KPS[a]	polystyrene	200 000	100	15	8.4×10^7	195 563	4.2	1296	94.3	1750	13.7	0.28
15%1.95MPS	polystyrene	1 950 000	15	22.8	4391	3821	10.7	3.1	0.13	2.5	23.8	0.47
40%349 KPI	polyisoprene	349 000	40	27	15 000	53 131	9.5	0.72	0.024	0.7	30	0.35
14%1MPI	polyisoprene	1 050 000	14	28.1	1000	6358	16.1	0.43	0.013	0.31	33.1	0.57
145 KPI	polyisoprene	145 000	100	28.8	60 000	350 865	5.9	0.43	0.013	0.5	33.1	0.20
390 KPS[a]	polystyrene	390 000	100	29.3	7.57×10^8	195 563	4.2	9678	288	9000	33.6	0.14
20%1.95MPS	polystyrene	1 950 000	20	30.4	16 446	6763	9.3	6.3	0.18	4.8	35	0.31
10%3.9MPS[b]	polystyrene	3 900 000	10	30.5	4415	1706	13.1	6.9	0.2	5.5	34.5	0.43
80%212 KPI	polyisoprene	212 000	80	33.4	93 500	220 433	6.6	1.04	0.026	1.0	40	0.20
15%3.9MPS[b]	polystyrene	3 900 000	15	45.7	45 314	3821	10.7	27.3	0.45	1.6	60.7	0.23
17%3.9MPS	polystyrene	3 900 000	17	51.7	118 500	4899	10.1	55.0	0.78	40.0	70.5	0.19
263 KPnBA	poly(*n*-butyl acrylate)	263 000	100	16.4	130 000	131 060	4.1	–	0.185	–	–	0.25

[a]Data taken from Bach et al.[4] at 130 °C. [b]Data taken from Bhattacharjee et al.[2]

apparent departure from expected behavior has motivated the discussion in this area, and although some efforts at reconciling the contradicting behaviors in regime 3 has been made on theoretical grounds,[5] the problem has remained essentially unresolved until date. More worryingly a review of the theoretical literature in this area would identify models that predict and justify both types of behaviors: one where the extensional viscosity increases above the value of $3\eta_0$ when the strain rate is of the order of the inverse of the Rouse time of the chains and the other where this behavior is not noticed.

Recently, two papers[6,7] appeared that have postulated that at high strain rates, there is a reduction of monomeric friction coefficient arising from orientation of the sub chains. This postulate was supported by experiments using birefringence data[5] and stress relaxation measurements,[6] which indicated an acceleration of chain relaxation. Incorporation of this friction reduction into a slip-link simulation[7] gave good agreement with data for polystyrene melt. Such a postulate could explain why polymer melts show no upturn in the extensional viscosity at high strain rates. For polystyrene solutions, it is argued that stress relaxation data does not exhibit accelerated decay over and beyond that expected by the Rouse process, which would signal a reduction in friction. Such a difference is attributed to the fact that the average subchain orientational anisotropy of the polymer and solvent is small. In the melt the stretched and oriented subchains are surrounded by similarly stretched material whereas in solutions the solvent surrounding the chains remains isotropic.

During the writing of this manuscript, the paper by Huang et al,[8] appeared. This showed, rather surprisingly, that concentrated polymer solutions are different from melts in extensional flow. This conclusion is based on data obtained using blends of polystyrene with oligomeric polystyrene. The experiments were conducted in melt state. The same polymer with three different oligomers[9] at similar volume fraction gave different extensional viscosities in regime 3. The authors conclude that nematic interactions between the solvent and the polymer lead to different reduction in the monomeric friction. Such nematic interactions are significant when the diluent is longer than a Kuhn segment. The other surprising result is that for these systems the extensional viscosity in regime 3 is nearly constant. In contrast to undiluted polystyrene melt where the viscosity continues to decrease. If nematic interactions were the cause of this behavior, it would imply that these interactions work to exactly cancel the effect of friction on the tube of equilibrium dimensions. This paper explores this issue in greater detail and shows that comparison with other polymer systems does not indicate any major difference between solutions and melts in other systems.

In view of the great interest that the above problem has generated, we intend here to provide a set of experimental data obtained earlier in our laboratoty,[10] and augmented by additional data that explores the role that the parameters Z, η_0, and λ_{max} play in influencing the relationship between stress and strain-rate. In the following, we have reported a large number of experiments on a variety of carefully constructed fluids to extract scaling relationships in various regimes. There are several advantages in using solutions to elucidate general trends. The ability to vary both concentration as well as molecular weight allows one to tailor solutions to explore a wider range of parameters than possible using polymer melts. Furthermore, operation at 21.5 °C negates any concern about thermal degradation of sample. We also note that existing literature is dominated by studies done using polystyrene. In this work we have therefore included extensional flow results for fluids containing other polymeric species to explore if changing the polymer to a molecule other than polystyrene actually affects the outcome of the experiments. Accordingly we have included results on polyisoprene (PI) and poly(*n*-butyl acrylate) (PnBA), in pure form as well as in solution, in filament-stretching experiments conducted at 21.5 °C. The glass transition temperatures of PI and PnBA are −70 and −49 °C respectively. Therefore, at 21.5 °C they are at least 91 and 70 °C above the glass transition temperature and can be considered as melts. To provide some perspective to these experiments, we note that the experiments reported by Bach et al.[4] on polystyrene melts were conducted at temperatures that exceed the glass transition temperature of polystyrene by a comparable amount. We will demonstrate that the extensional viscosity increases beyond its Newtonian value of $3\eta_0$ when the strain rate is of the order of the inverse of the Rouse time of the chains not only in entangled solutions of polystyrene but also in those of PI and PnBA based fluids. In this way we will demonstrate that the extensional flow behavior in regime 3 is qualitatively identical in all examined cases irrespective of the details of the structure of the polymer chains. Additionally, we have demonstrated that under certain conditions the extensional flow characteristics can be normalized to collapse the

dx.doi.org/10.1021/ma401213r | Macromolecules 2014, 47, 379−386

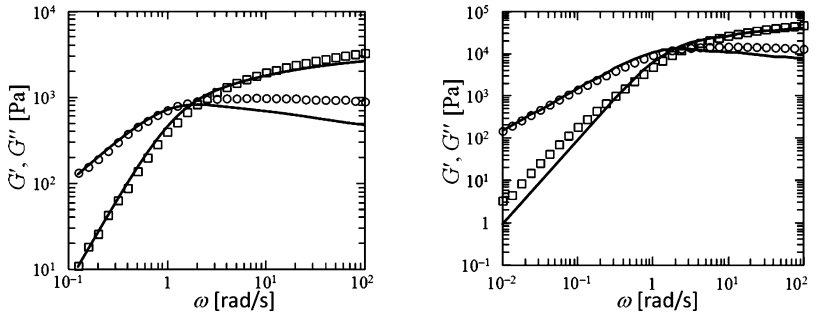

Figure 1. G' (squares) and G'' (circles) data along with the Milner−Mcleish model predictions (solid lines) for (a) 14%1MPI solution and (b) 40%349 KPI solution.

experimental data across all three regimes that we can access in experiments. We hope that our contribution can serve as a guide for future modeling efforts.

II. EXPERIMENTAL SECTION

The rheological properties of entangled polymeric fluid are governed primarily by the number of entanglements per chain (Z) and the finite extensibility of the chains that is characterized by the maximum stretch ratio λ_{max}. Therefore, we have used solutions where these parameters can be systematically varied. Solutions of various concentrations were produced by dissolving the polymers of interest in a suitable "high-boiling-point" (>200 °C) solvent and in presence of a volatile cosolvent. Following thorough mixing of the components the cosolvent was slowly evaporated out of the system. In this way a stable homogeneous solution of the polymer in a chosen solvent was obtained.

We have used six polymeric fluids which span three different polymeric species including polyisoprene (PI), poly(*n*-butyl acrylate) (PnBA), and polystyrene (PS). The polymers were obtained from Polymer Source (Canada) and had a polydispersity index ranging from 1.05 to 1.14 and hence it is not expected that polydispersity has an effect on the data reported here. The glass transition temperature of PI and PnBA are −70 and −49 °C respectively. Therefore, in pure form we consider them as melts at 21.5 °C We have used various molecular weights of PI so that the flow behavior can be considered for the same species in a melt and a solution with near identical number of entanglements (Z) per chain, as well as among solutions having varying degrees of entanglement. The PI solutions are constituted in squalane using chloroform as a cosolvent. Polystyrene solutions were constituted in diethyl phthalate (DEP) using methylene chloride as a cosolvent. The solvents and cosolvents were of analytical grade and obtained from Sigma-Aldrich, USA. Table 1 lists the details of the fluids used in this work.

III. MATERIAL PARAMETERS AND TIME CONSTANTS

The material parameters of the underlined fluids in Table 1 were obtained from literature sources that are cited below the table. All other fluids were subjected to small amplitude oscillatory shear flow in this work to obtain the linear viscoelastic response and the results were used to estimate the time constants τ_d^f and τ_R by fitting the experimental data to the predictions of the Milner−McLeish model.[11] The Milner−McLeish model predicts the linear viscoelastic behavior of entangled systems of linear polymers once the plateau modulus (G_N^0) and the number of entanglements per chains (Z) are known. These parameters can be estimated using well established correlations[12] and measurable properties like the density (ρ), stiffness of the chain (C_∞) and the molecular weight between entanglements in a melt (Me). For melts of the polymers used here, values of these parameters are available: for PI, C_∞= 5, Me = 5027 and ρ = 0.9 g/cm^3 and for PS C_∞= 9.6, Me = 13300 and ρ = 1.07 g/cm^3. The parameters for PnBA carry some uncertainty. Estimates for $C_\infty$are interpolated using data for 3 poly(alkyl acrylates) given by Fetters et al.[13] G_N^0 is estimated from dynamic data, from the value of G' at the minimum of the loss modulus, G''. Another estimate was also obtained using correlation between G_N^0 and the modulus at the cross over frequency for a large number of systems published in the literature. Both these gave similar values for PnBA, C_∞= 10.2, Me = 16000 and ρ = 1.08 g/cm^3. It is readily admitted that these estimates involve larger uncertainty for PnBA than other systems. For concentrated, entangled solutions the molecular weight between entanglements Me_{soln} was estimated using a dilution rule $Me_{soln} = Me(c/\rho)^{-1}$ and the corresponding plateau modulus is estimated as $G_N^0 = (4cRT/5Me_{soln})$. Additionally the number of entanglements per chain was calculated as $Z = M_w/Me_{soln}$ where M_w is the molecular weight of the polymer chain. The developments and arguments that lead to these correlations are provided in ref 12 and are not further discussed here. For the present it suffices to state that the values of Z and G_N^0 are used in conjunction with the Milner−McLeish model to estimate the time constants of the fluid. The procedure involves treating the segmental relaxation time, τ_e, in the model as an adjustable parameter and altering it to obtain the best agreement between the predicted and measured loss modulus values in the low frequency region. Parts a and b of Figure 1 show representative fits to the experimental linear viscoelastic data. In comparing these dynamic data to melt data appearing in the literature, it is worthwhile emphasizing that these are data at a single temperature without the aid of time−temperature superposition to expand the frequency range. The relaxation times are then calculated using the correlation $\tau_d^f = 3Z\tau_R(1 - 2s_d)^2 = 3Z^3\tau_e(1 - 2s_d)^2$, where s_d is a parameter that arises in the Milner−McLeish model and depends on Z. The details of the model are available in the origin work of Milner and McLeish[11] and are not further discussed here. In addition to Z, G_N^0 and the time constants we also estimates the maximum stretch ratio which is the ratio of total (maximum) length to the equilibrium length of the polymer chain and is given by $\lambda_{max} = (N_K/Z)^{1/2}$ where N_K is the number of Kuhn steps in the chain. These estimates are also listed in Table 1.

dx.doi.org/10.1021/ma401213r | *Macromolecules* 2014, 47, 379−386

IV. EXTENSIONAL RHEOLOGY

The extensional flow experiments were carried out using the filament stretching rheometer proposed by Sridhar et al.[13] and Tirtaatmadja and Sridhar.[14] In the current design a small sample of the test fluid is held between two parallel plates, 3 mm in diameter, that are moved apart in a manner such that the center of the filament undergoes ideal, homogeneous, uniaxial deformation. By controlling the displacement profile, the strain rate can be controlled. The tensile force is measured by a transducer (Transducer Techniques, USA) at the top end plate and the filament diameter at the midplane is monitored by a laser micrometer (Zumbach, Germany) or by high-speed photography using a Phantom V5 (Vision Research, USA) camera that is capable of collecting data at 1000 frames-per-second at 1024 × 1024 pixels (approximately 10 μm per pixel) resolution. Using the information on the temporal variation of the midfilament diameter and the force, the extensional viscosity can be calculated by well-established procedures.[15] The experiments discussed in this work are conducted in the "rate-controlled" mode at 21.5 °C. During experiments care was taken to eliminate decohesion at the end plate by either gluing the material (145 KPI and 80%212kPI) to the end plate using fast curing epoxy (Araldite Selleys, NSW, Australia). Also optical microscopy was used to monitor sagging of the filaments at low stretch rates. Experiments reported here were not affected by sagging.

In this paper, we are mainly focusing on steady state extensional viscosity. We have previously published data on the PS solutions.[16] A sample plot of the start up of steady extensional viscosity is shown in Figure 2 for the 200 KPnBA

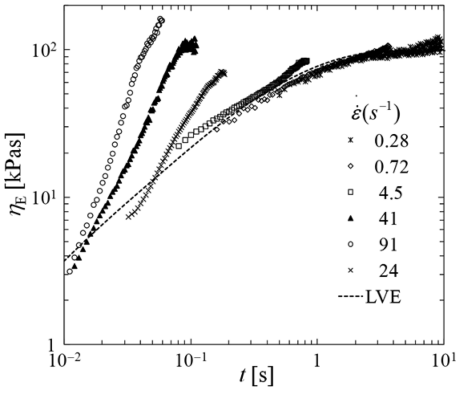

Figure 2. Start up of steady extension at various strain rates for the 200 KPnBA melt. The dashed line is the linear viscoelastic envelope.

system. A constant viscosity was obtained for at least 0.5 strain units for the highest strain rates and 1−2 strain units for moderate strain rates and indicated the steady state in extensional viscosity. At the lowest strain rates the data are consistent with the predictions of linear viscoelasticity shown as a dashed line on the figure. It was however not possible to access strains and strain-rates that are high enough to observe the saturation of the extensional viscosity that is expected to occur in regime 4 due to the limitations on the highest achievable strain rate and velocity in the present instrument. Thus, the response of the fluids in this regime was not studied in this work.

V. RESULTS

Appropriate normalization of the variables is essential while comparing the rheological response of various polymeric systems. Conventionally, the extensional viscosity is normalized to Trouton ratio (Tr) with the zero shear viscosity. Tr shifts all the data sets vertically onto a common value of 3 at the low extension rate end. The rate of extension can be made nondimensional by the use of a relaxation time. Several relaxation times are available for this purpose leading to different Weissenberg numbers (Wi). The Weissenberg numbers shifts the data horizontally to an extent that depends on the choice of the relaxation time. Parts a and b of Figure 3 present the Trouton ratio vs Weissenberg number data. In the Figure 3a, τ_d^f the effective reptation time is chosen to normalize the extension rate. The resulting Weissenberg number is denoted as $Wi_{\tau_d^f}$ In such representation, the transition from constant viscosity Regime 1 to extension thinning regime 2 occurs at $Wi_{\tau_d^f} \approx 1$. It is clear from Figure 3a that all the data sets, except 200 KPnBA, superimpose in the extension-thinning regime and show an upturn at different values of $Wi_{\tau_d^f}$ depending on the respective τ_R. In Figure 3b, the Weissenberg number is calculated based on Rouse time (denoted as $Wi_{\tau R}$). In this representation the curves are shifted such that all of them show an upturn at $Wi_{\tau R} \approx 1$. This is consistent with the onset of chain stretching at the beginning of Regime 3. It also suggests that the estimate of Rouse time, obtained through the procedure used in this work is reasonable.

In the Figure 4, nondimensional plots of steady state stress against extension rate are presented. The extensional stress is normalized by the plateau modulus, G_N^0. The extension rate is made nondimensional using the relaxation time chosen based on the flow regime under consideration.

In regime 1, the mechanism of pure reptation is known to dominate the dynamics of relaxation. Hence, the effective reptation time, τ_d^f is chosen to normalize the rate of extension while comparing the experimental data in the Regime 1 (resulting Weissenberg numbers represented as $Wi_{\tau_d^f}$). In Figure 4a, the experimental data of all the systems, corresponding to the first regime are presented. It is clear that all the data sets collapse onto a common trend of slope 1. regime 1 ends at $Wi_{\tau_d^f} \approx 1$ where the stresses reach G_N^0. The stress equals the plateau modulus as a result of the complete alignment of the tubes in the direction of the flow. From Figure 4a, it can be inferred that all the entangled polymeric systems studied display the identical trend in regime 1.

Regime 2 spans between extension rates equal to $1/\tau_d^f$(beyond which reptation is frozen) and $1/\tau_R$ (where the chain stretching is anticipated to set in). In regime 2, the distribution of chain orientations which is Gaussian in regime 1, becomes narrower as the Wi increases. While flow aligns the chains, the convective constraint release (CCR) mechanism causes diffusion of chain orientation and loss of entanglements. Width of regime 2 depends on the separation of time scales τ_d^f and τ_R. It is known that the reptation time τ_d^f scales approximately as $Z^{3.4}$ (Z is the number of entanglements per chain) and Rouse time τ_R as $\sim Z^2$. Accordingly, the window of regime 2 scales as $Z^{1.4}$. While examining the rheological response of the entangled systems in regime 2, the systems with nearly equal number of entanglements per chain have been grouped together. The Weissenberg number is evaluated based on τ_d^f.

dx.doi.org/10.1021/ma401213r | Macromolecules 2014, 47, 379−386

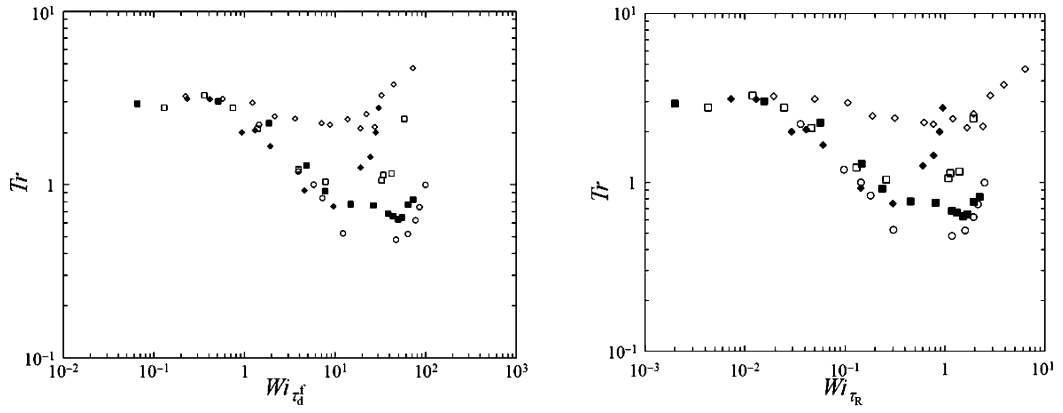

Figure 3. Trouton ratio vs Weissenberg number. The extension rate is nondimensionalised by (a) the reptation time with the effect of CLF. (b) The Rouse time. The symbols correspond to: open diamonds, 200 KPnBA; closed diamonds, 14%1MPI; open squares, 40%349 KPI; closed squares, 145 KPI; circles, 80% 212 KPI.

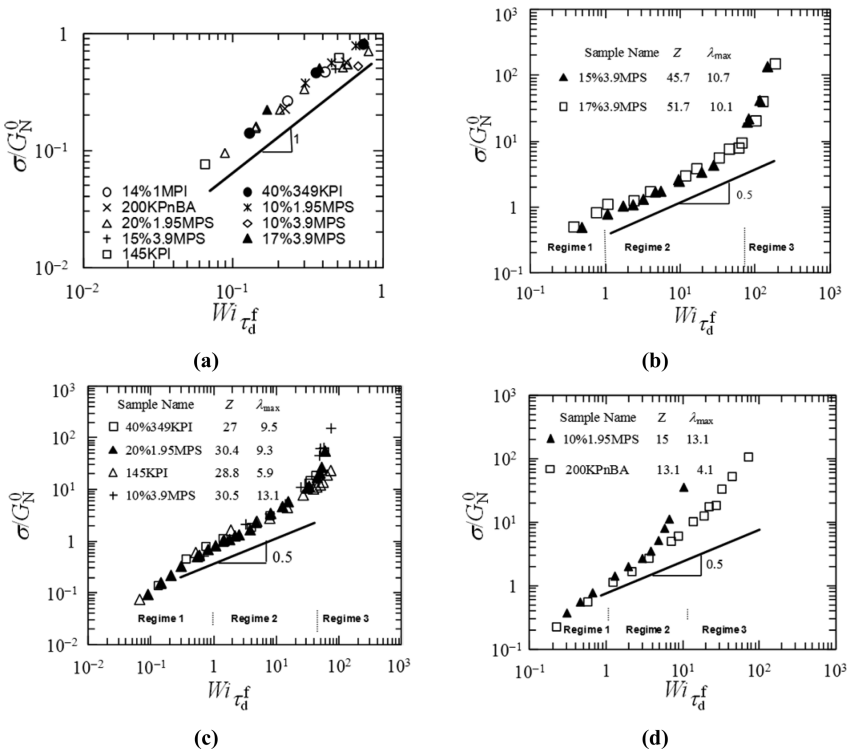

Figure 4. Nondimensionalised stress vs Weissenberg number based on. τ_d^f: (a) regime 1, $Wi_{\tau_d^f} < 1$ (b) highly entangled, (c) moderately entangled and (d) lightly entangled polymeric systems, with the slope of regime 2 highlighted.

In the Figure 4b, experimental data of the systems with high number of entanglements ($Z \sim 50$) are plotted together. In this case, the data in regime 2 span over 2 decades in Weissenberg number. The systems clearly exhibit the slope of 0.5 (beyond $Wi_{\tau_d^f} \approx 1$) in this regime. In Figure 4c, the systems with moderate number of entanglements ($Z \sim 30$) per chain have been grouped. With the smaller number of entanglements the window of regime 2 gets narrower. It is also observed that the effect of chain-stretch extends into regime 2. With a moderate Z, one finds that the initial slope in regime 2 is also 0.5. The slope gradually increases as the Weissenberg number increases. Hence, the average slope of the curve in regime 2 appears to be slightly higher than 0.5. The onset of the chain stretch is observed to depend on the maximum chain stretch ratio (λ_{max}). In Figure 4c, the systems with higher λ_{max} display early chain stretch. Such a trend suggests that more flexible systems (those with higher λ_{max}) undergo chain stretch at lower strain rates. Early effect of chain stretch is also exhibited by the systems with small number of entanglements per chain. In Figure 4d, the data corresponding to lightly entangled ($Z \sim 15$) polymeric systems are shown. In these sets of data, regime 2 is hardly noticed. The effect of chain stretch extends well into the regime 2 making it difficult to demarcate the onset of regime 3 in the stress plots. Thus, the width of the window of regime 2 is dependent on the value of Z and the onset of regime 3 is affected by the value of λ_{max}. Simulations[17] show that at lower

dx.doi.org/10.1021/ma401213r | *Macromolecules* 2014, 47, 379−386

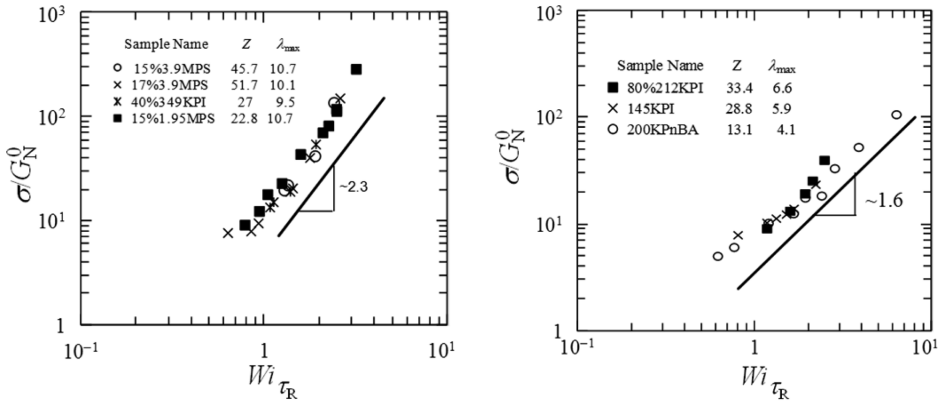

Figure 5. Regime 3 ($Wi_{\tau R} > 1$) of the steady state stress plots of the polymeric systems with (a) high λ_{max} values and (b) low λ_{max} values. The systems vary in their number entanglements per chain.

Z, the distribution of orientation is strongly peaked even at a lower wi, indicating the earlier onset of chain stretching.

In regime 2, constraint release has the dominant effect. Simulations[17] show that entanglements are washed out as a result of diffusive and convective processes. The actual number of entanglements under these conditions may be 50% of the number at equilibrium conditions. Hence lightly entangled systems at the start are hardly entangled when they reach steady stretching under these flow conditions.

Regime 3 is best described using the Weissenberg number based on Rouse time, τ_R ($Wi_{\tau R}$). In parts a and b of Figures 5, the nondimensional stress (σ/G_N^0) vs Weissenberg number plots (corresponding to $Wi_{\tau R} > 1$) of various entangled polymeric systems are presented for regime 3. While in regime 2, the orientation of the chains is the dominant contributor to the stress, in regime 3 the stretch distribution becomes skewed and makes an increasing contribution to stress. While comparing the rheological response of the systems in regime 3, the data sets have been sorted based on their values of λ_{max}. In Figure 5a, systems whose λ_{max} values range from 9.5 to 10.7 have been presented. Figure 5b shows the systems with lower λ_{max} values (4.1−6.6). Collapse of the data sets suggests that the Rouse time controls the mechanism of chain stretch. A higher slope observed in the case of larger values of λ_{max} suggests that the rate of chain stretch is dependent on the flexibility of the chain. Transition from regime 2 to regime 3 occurs gradually near $Wi_{\tau R} \sim 1$. It is also noted that the steady state stress is larger than 10 times the plateau modulus in the chain stretch regime

The trends exhibited by the entangled polymeric systems, as described above, are consistent with Doi−Edwards tube model along with the chain stretch mechanism.[18] The trend observed in regime 2 also supports the DE model with interchain pressure effect proposed by Marrucci et al.[5] with the slope of 0.5.

In an alternative representation of the steady state stress data, σ/G_N^0 is plotted against the Weissenberg number evaluated based on the tube deformation relaxation time, τ_p. The tube deformation relaxation time, τ_p, is defined by Marrucci et al. in their tube model with the interchain pressure effect.[5] As mentioned earlier, τ_p is estimated to be the inverse of the extension rate at which the steady state extension stress becomes equal to the plateau modulus. Thus, τ_p is deduced from the experimental extensional data unlike τ_d^f and τ_R which are obtained as the model fitting parameters to the dynamic data. The value of τ_p is not a model dependent. As per definition of τ_p, it forces the stress curves to pass through the point where $Wi_{\tau p} = \sigma/G_N^0 = 1$.

In Figure 6, the nondimensional stress vs $Wi_{\tau p}$ plots of the entangled systems studied in the present work are shown. An

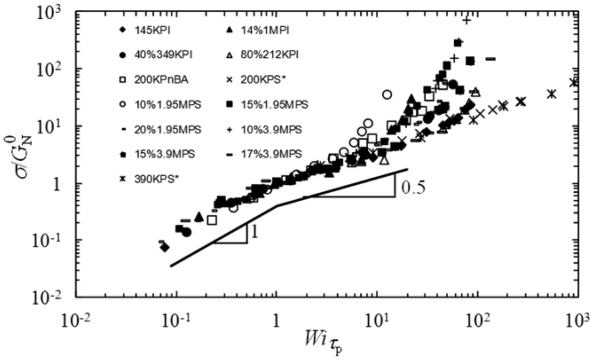

Figure 6. Steady state elongational stress (σ) nondimensionalised by the plateau modulus (G_N^0) plotted against Wi, extension rate nondimensionalised by τ_p, for various systems studied in the present work.

interesting observation made in this representation is that the systems with nearly equal values of λ_{max}/Z collapse on each other in all the three regimes. In parts a and b of Figure 7, systems with equal values of λ_{max}/Z have been grouped and the data superimposed, suggesting that λ_{max}/Z is the dominant parameter.

It is also noticed that the systems with larger value of λ_{max}/Z show an earlier upturn in the stress vs extension rate plot leading to the suggestion that chain stretching occurs at a lower strain rate for these systems. Accordingly, the systems with smaller value of λ_{max}/Z display a slope ~0.5 for wider range of $Wi_{\tau p}$. In Figure 6, the uniaxial extensional stress data on monodisperse polystyrene melts have also been presented. G_N^0 and τ_p for PS melts are evaluated in the manner similar to that followed for systems studied in the present work. Hence the values of the parameters differ slightly from those presented in the publication of Bach et al.[4] Table 1 also lists the parameters of polystyrene melts studied by Bach et al.,[4] as evaluated by the method discussed above. It is clear from the Figure 6 that the Polystyrene melts do not show a perceptible upturn in the stress-plots. The regime with slope ~0.5 extends over the entire

dx.doi.org/10.1021/ma401213r | Macromolecules 2014, 47, 379−386

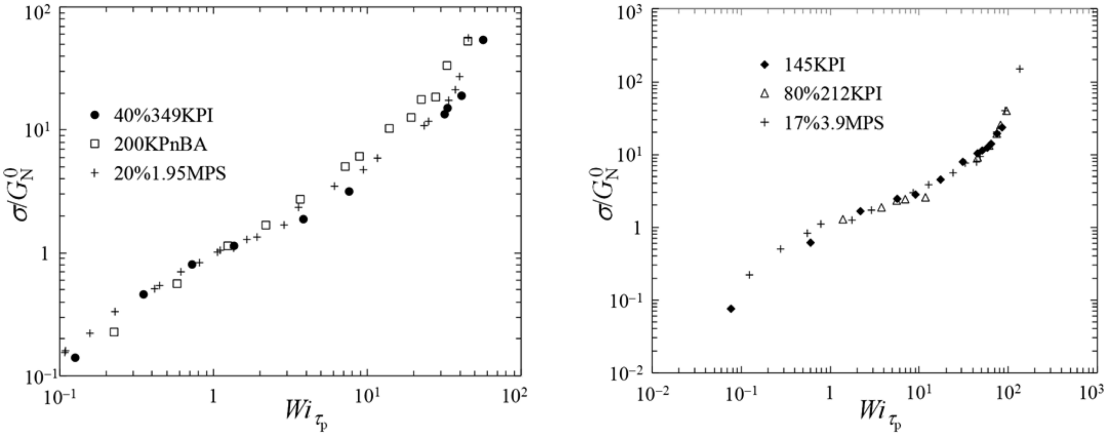

Figure 7. Steady state elongational stress (σ) nondimensionalized by the plateau modulus (G_N^0) plotted against Wi, extension rate nondimensionalized by τ_p, for various systems studied in the present work.

range of Wi probed by the experiments. Considering the parameter λ_{max}/Z of the polystyrene melts, 200 KPS melts ($\lambda_{max}/Z = 0.28$) should fall close to 145 KPI melt and 80%212 K PI solution ($\lambda_{max}/Z = 0.2$). The fact that λ_{max}/Z emerges as a parameter is rather surprising. The significance of λ_{max}/Z in determining the chain stretch is not entirely clear and is presented as an empirical observation. Simulations are required to throw further light on this.

It is useful to compare existing results so that key points of difference between polymer systems can be elaborated. Figure 8

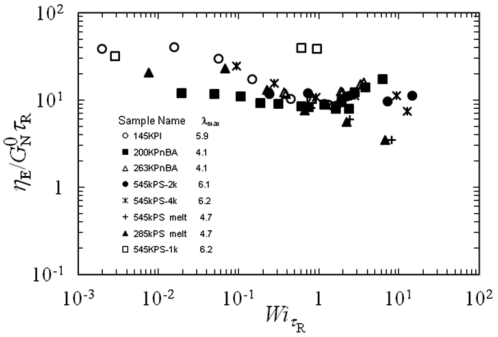

Figure 8. Extensional viscosity of PI, PnBA, and PS (diluted by oligomers) as a function of Wi showing different behavior in regime 3.

shows a comparison of the extensional viscosity of various systems. All these have been processed in the melt state. There are three different pattern emerging from this comparison. PI and PnBA show an increase in viscosity beyond a $Wi_{\tau R}$ of approximately 1 and these could be termed as consistent with tube theory. The polystyrene melts continue to decrease beyond $Wi_{\tau R} \sim 1$ and this has been commented on earlier. As mentioned earlier, reduction in monomeric friction due to chain anisotropy has been advanced as a reason for lack of chain stretching. Since the number of Kuhn segments in an entanglement strand in PI is larger than in PS, it is argued that PI is susceptible to chain stretching prior to chain orientation. However, PnBA has a similar number of Kuhn steps per entanglement to PS, yet its behavior follows that of PI. PS and PnBA have similar backbone structure with a C−C bond whereas PI has a C═C bond in the backbone.

However the number of entanglements for PnBA is less than PS melt, and it is plausible that at steady state PnBA is only lightly entangled due to CCR effects in removing entanglements. It is obvious that a number of competing effects transform the sample being deformed and the state of the deformed sample at steady state is quite different from that at equilibrium. The suggested diagnostic for the reduction in friction is that the stress relaxation after cessation of stretching would shows acceleration in relaxation due to orientational anisotropy. Figure 9 presents such a diagnostic for PnBA

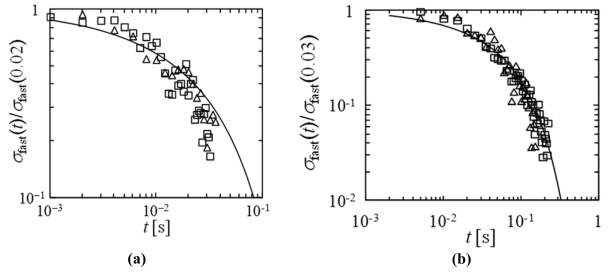

Figure 9. Stress relaxation melt after cessation of extensional deformation. (a) 200 KPnBA: squares, $\varepsilon = 2.7$, $Wi_{\tau R}= 3.7$; triangles, $\varepsilon = 2.8$, $Wi_{\tau R}= 2.2$. (b) 263 KPnBA: triangles: $\varepsilon = 3.6$; $Wi_{\tau R}= 2.2$; Circles: $\varepsilon = 3.7$; $Wi_{\tau R}= 3.3$; line is the Rouse relaxation.

following the protocol advanced by Yaoita et al.[7] This figure shows the relaxation measured using the technique described by Bhattacharjee et al.[2] The relaxation stress after cessation of stretching is corrected for the contribution of the terminal relaxation process associated with reptation. The stress relaxation at different $Wi_{\tau R}$ follows the Rouse relaxation and this is consistent with its behavior in Figure 8. Hence according to the idea advanced by ref 7, there is no reduction in monomeric friction due to orientation and stretching. Finally the PS systems with a diluent in the form of an oligomer show an entirely different trend. The extensional viscosity beyond $Wi_{\tau R} \sim 1$ is nearly constant. This has been attributed[9] to nematic interactions between the oligomer and the polymer chain.

Clearly *a priori* prediction of behavior under these conditions through conventional chain model parameters remains a challenge.

dx.doi.org/10.1021/ma401213r | *Macromolecules* 2014, 47, 379−386

VI. CONCLUSIONS

It is clear from the available literature that very little experimental work has been carried out in the field of extensional rheometry. The data presented in this paper adds to the pool of uniaxial extensional stress growth data of entangled polymeric systems. The existing data on entangled polymeric systems is dominated by polystyrene (PS) systems. Thus, the characterization of polyisoprene (PI) and poly(*n*-butyl acrylate) (PnBA) broadens the range of materials being studied. However, at the time and length scales at which rheological characterization is done, it is argued that the microstructure of the polymer should not matter. Similar rheological response of PI and PnBA systems as well as that of the concentrated solutions of PS substantiates this argument.

The main motivation for the present work has been the observed divergence in the rheological response of concentrated Polystyrene solutions and melts under uniaxial extensional flow.[4,14] The results presented above clearly show that the concentrated polymeric solutions and melts do display identical rheological response when subjected to homogeneous uniaxial extensional flow. Monodisperse polymeric melts of polyisoprene and poly(*n*-butyl acrylate) along with few concentrated solutions of PI have been tested using the filament stretching rheometer. All the tests are carried out at 21.5 °C which avoids the risk of degradation or oxidation.

In contrast to the data of polystyrene melts,[4] the polyisoprene as well as poly(*n*-butyl acrylate) melts show an upturn in the steady state viscosity at an extension rate equal to $1/\tau_R$. Such upturn has previously been reported in case of polystyrene solutions and similar trend has been reported in this work for three other polyisoprene solutions. This proves that the concentrated polymeric solutions and entangled melts exhibit identical rheological response. However, the cause for the absence of upturn in extensional viscosity curves of polystyrene melts remains unknown.

There are clearly different types of behaviors in regime 3. PI both melt and in solutions, PnBA in melt state, and PS in a solution all show similar trend with the viscosity increasing and consistent with the predictions of the tube theory. PS melts shows that the viscosity continues to decrease in regime 3. When PS is diluted with oligomers and tested in the melt state, the viscosity remains constant in regime 3. While some suggestions have been advanced to explain some of these effects, reconciling these differences *a priori* in terms of the tube theory remains a challenge.

By normalizing the steady state stress with the plateau modulus, G_N^0 and the strain rate by the tube deformation relaxation time, τ_p, an interesting observation has been made. In such representation, the systems with nearly equal values of λ_{max}/Z collapse on each other in all the three regimes. None of the existing molecular models yield such a parameter upon rearrangement/simplification. By rewriting λ_{max}/Z in terms of more basic parameter such as N_K ($\lambda_{max}/Z = N_K^{1.5}/Z^{0.5}$) it can be related to the flexibility of the polymeric system. Higher the value of λ_{max}/Z; more is the flexibility of the system; hence the early upturn in the stress plots. However, we admit that this does not provide a comprehensive explanation of the parameter λ_{max}/Z. Hence, we present this argument just as empiricism.

AUTHOR INFORMATION

Corresponding Author

*E-mail: (T.S.) tam.sridhar@monash.edu.

Notes

The authors declare no competing financial interest.

ACKNOWLEDGMENTS

The work described in this paper was supported by a grant from the Australian Research Council. We acknowledge some useful comments by the reviewers.

REFERENCES

(1) Doi, M.; Edwards, S. F., *The theory of polymer dynamics*; Oxford University Press: Oxford, U.K., 1986.
(2) Bhattacharjee, P. K.; Nguyen, D. A.; McKinley, G. H.; Sridhar, T. *J. Rheol.* **2003**, *47*, 269−290.
(3) Bhattacharjee, P. K.; Oberhauser, J. P.; McKinley, G. H.; Leal, L. G.; Sridhar, T. *Macromolecules* **2002**, *35*, 10131−10148.
(4) Bach, A.; Almdal, K.; Rasmussen, H. K.; Hassager, O. *Macromolecules* **2003**, *36*, 5174−5179.
(5) Marrucci, G.; Ianniruberto, G. *Macromolecules* **2004**, *37*, 3934−3942.
(6) Ianniruberto, G.; Brasiello, A.; Marrucci, G. *Macromolecules* **2012**, *45*, 8058−8066.
(7) Yaoita, T.; Isaki, T.; Masabuchi, Y.; Watanabe, H.; Ianniruberto, G.; Marrucci, G. *Macromolecules* **2012**, *45*, 2773−2782.
(8) Huang, Q.; Mednova, O.; Rasmussen, H. K.; Alvarez, N. J.; Skov, A. L.; Hassager, O. *Macromolecules* **2013**, *46*, 5026−5035.
(9) Huang, Q.; Alvarez, N. J.; Matsumiya, Y.; Rasmussen, H. K.; Watanabe, H.; Hassager, O. *ACS Macro Letter* **2013**, *2*, 741−744.
(10) Acharya, M. V.; Bhattacharjee, P. K.; Nguyen, D. A.; Sridhar, T. *Proceedings of the 15th International Congress on Rheology*; AIP: Melville, NY, 2008.
(11) Milner, S. T.; McLeish, T. C. B. *Phys. Rev. Lett.* **1998**, *81*, 725−728.
(12) Larson, R. G.; Sridhar, T.; Leal, L. G.; Mckinley, G. H.; Likhtman, A. E.; McLeish, T. C. B. *J. Rheol.* **2003**, *47*, 808−818.
(13) Fetters, L. J.; Lohse, D. J.; Colby, R. H. *Physical properties of polymers handbook*; Mark, J. E., Ed.; Springer: Berlin, 2006.
(14) Sridhar, T.; Tirtaatmadja, V.; Nguyen, D.; Gupta, R. *J. Non-Newtonian Fluid Mech.* **1991**, *40*, 271−280.
(15) Tirtaatmadja, V.; Sridhar, T. *J. Rheol.* **1993**, *37*, 1081−1102.
(16) Mckinley, G. H.; Sridhar, V. *Annu. Rev. Fluid Mech.* **2002**, *34*, 1305−1318.
(17) Kushwaha, A.; Shaqfeh, E. S. G. *J. Rheol.* **2011**, *55*, 463−483.
(18) Marrucci, G.; Ianniruberto, G. *J. Rheol.* **2001**, *45*, 1305−1318.